

Energy-efficient and precise trajectory-tracking with bracing manipulator

Daisuke Kondo¹, Mamoru Minami¹, Xiang Li¹ and Akira Yanou¹

¹ Okayama University, Japan

(Tel: 81-86-251-8924)

¹en421835@s.okayama-u.ac.jp

Abstract: Considering that humans perform handwriting task with small powers by contacting elbow or wrist on a table, it is reasonable to deem that manipulators can save energy and simultaneously accomplish trajectory tracking tasks precisely like humans by bracing intermediate links. First this paper discusses equation of motion of robot under bracing condition, based on the robot's dynamics with constraint condition including motor dynamics. Then this paper propose to control simultaneously bracing force and hand's trajectory tracking, followed by optimization of the elbow-bracing position that minimizes energy consumption.

Keywords: Manipulator, Constraint Motion, Energy Saving

1 INTRODUCTION

Redundant manipulators based on kinematics have been researched widely and the effect is introduced by Chirikjian and Burdick [1]. Hyper-redundant manipulators can variedly change the configuration through the use of the redundancy. But, the weight of manipulators with high redundancy increase as the number of links increases. Then, weight capacity of the hand is lessened. In many researches, methods of using redundancy such as obstacle avoidance [2, 3] and optimization of configuration [4] were discussed, and have been used practically in factories. But hyper-redundant manipulators do not reach practical level at the present stage.

As Fig.1 is shown, humans can accurately write characters with less power for writing motions. Redundant manipulators have possibilities to save energy and work accurately by bracing elbow on environments.

Effectiveness and accuracy of hyper-redundant manipulator subject to constraint on environments have been discussed, West and Asada [5] proposed common contact mode of kinematics for designing position/force simultaneous controller of manipulator subject to constraint.

In this report, we consider the control method of undeformable robots and undeformable environments. Under these conditions, algebraic equation can be derived from constraint condition and equation of motion as Eq.(1).

$$A\mathbf{f}_n = \mathbf{a} - B\boldsymbol{\tau} \quad (1)$$

\mathbf{f}_n is constraint force, A , \mathbf{a} and B are vector and matrices that will be defined in the next chapter, $\boldsymbol{\tau}$ is vector of input torques. Eq.(1) shows an algebraic relation between input torques and constraint force when robot's hand is subject to constraint. The above equation has been derived by Hemami [6] in discipline of biped walking, and applied by Peng [7] in discipline of force/position control by robots at



Fig. 1. Human's writing motion

the beginning. Peng considered that $\boldsymbol{\tau}$ is input and \mathbf{f}_n is output, and Eq.(1) was used as force sensor to detect \mathbf{f}_n . In this paper, Eq.(1) is used as figuring input torque to accomplish desired constraint force \mathbf{f}_{nd} by contraries. Considering the hand writing motion, we know that too much pushing one's wrist to table in tiring, and also too less pushing makes us tiring too. This means that appropriate supporting force generated from table when bracing wrist or elbow, exists.

Authors propose control method of controlling constraint force, hand position and elbow position simultaneously in constraint motion and analyze effectiveness of constraint motion through trajectory tracking of the hand and energy consumption. Moreover, we optimize bracing position and hand's load based on minimization criterion of energy, and discuss the relation between optimal bracing position, hand target trajectory and hand's load.

2 MODELING WITH CONSTRAINT MOTION

2.1 Constraint motion with bracing elbow

In this section, we make a model an elbow-bracing robot that contacts multiple points with environments. Considering conditions that intermediate links of of a n -link manipulator

are subject to constraint at p points. Constraint condition is expressed as,

$$\begin{aligned} C(\mathbf{r}(\mathbf{q})) &= [C_1(\mathbf{r}_1(\mathbf{q})), C_2(\mathbf{r}_2(\mathbf{q})), \dots, C_p(\mathbf{r}_p(\mathbf{q}))]^T \\ &= \mathbf{0}. \end{aligned} \quad (2)$$

Here, \mathbf{q} is joint angle vector with n joints, \mathbf{r}_i is i -th link position that is subject to constraint. The relation between \mathbf{r}_i and \mathbf{q} and the relation between $\dot{\mathbf{r}}_i$ and $\dot{\mathbf{q}}$ are expressed as,

$$\mathbf{r}_i = \mathbf{r}_i(\mathbf{q}) \quad (3)$$

$$\dot{\mathbf{r}}_i = \mathbf{J}_i(\mathbf{q})\dot{\mathbf{q}}, \quad \mathbf{J}_i(\mathbf{q}) = [\tilde{\mathbf{J}}_i(\mathbf{q}), \mathbf{0}]. \quad (4)$$

In Eq.(4), \mathbf{J}_i is $m \times n$ matrix, $\tilde{\mathbf{J}}_i$ consists of $m \times i$ matrix and zero submatrix $\mathbf{0}$ is $m \times (n - i)$.

In this report, we consider that a case with a manipulation contacting plural points, and coefficient vectors that show direction of action of constraint forces and friction forces are $n \times 1$ vectors like

$$\left(\frac{\partial C_i}{\partial \mathbf{q}^T} \right)^T / \left\| \frac{\partial C_i}{\partial \mathbf{r}^T} \right\| = \mathbf{j}_{ci}^T \quad (5)$$

$$\left(\frac{\partial \mathbf{r}_i}{\partial \mathbf{q}^T} \right)^T \frac{\dot{\mathbf{r}}_i}{\|\dot{\mathbf{r}}_i\|} = \mathbf{j}_{ti}^T. \quad (6)$$

Moreover, \mathbf{J}_c^T , \mathbf{J}_t^T , \mathbf{f}_n and \mathbf{f}_t are

$$\mathbf{J}_c^T = [\mathbf{j}_{c1}^T, \mathbf{j}_{c2}^T, \dots, \mathbf{j}_{cp}^T], \quad (7)$$

$$\mathbf{J}_t^T = [\mathbf{j}_{t1}^T, \mathbf{j}_{t2}^T, \dots, \mathbf{j}_{tp}^T], \quad (8)$$

$$\mathbf{f}_n = [f_{n1}, f_{n2}, \dots, f_{np}]^T, \quad (9)$$

$$\mathbf{f}_t = [f_{t1}, f_{t2}, \dots, f_{tp}]^T. \quad (10)$$

\mathbf{J}_c^T , \mathbf{J}_t^T are $n \times p$ matrices, and \mathbf{f}_n , \mathbf{f}_t are $p \times 1$ vectors. Using above definitions, equation of motion of the manipulator subject to constraint at p points is expressed as

$$\begin{aligned} &M(\mathbf{q})\ddot{\mathbf{q}} + \mathbf{h}(\mathbf{q}, \dot{\mathbf{q}}) + \mathbf{g}(\mathbf{q}) + D\dot{\mathbf{q}} \\ &= \boldsymbol{\tau} + \sum_{i=1}^p (\mathbf{j}_{ci}^T f_{ni}) - \sum_{i=1}^p (\mathbf{j}_{ti}^T f_{ti}) \\ &= \boldsymbol{\tau} + \mathbf{J}_c^T \mathbf{f}_n - \mathbf{J}_t^T \mathbf{f}_t. \end{aligned} \quad (11)$$

Differentiating Eq.(2) with respect to time t twice, constraint condition of $\ddot{\mathbf{q}}$ is set up like

$$\dot{\mathbf{q}}^T \left[\frac{\partial}{\partial \mathbf{q}} \left(\frac{\partial C}{\partial \mathbf{q}^T} \right) \right] \dot{\mathbf{q}} + \left(\frac{\partial C}{\partial \mathbf{q}^T} \right) \ddot{\mathbf{q}} = \mathbf{0}. \quad (12)$$

The solution of Eq.(11) must satisfy Eq.(2) independently of time t that the manipulator be always subject to constraint. When $\ddot{\mathbf{q}}$ satisfying Eq.(12) is obtained and $\ddot{\mathbf{q}}$ in Eq.(11) keeps same value to the $\ddot{\mathbf{q}}$ in Eq.(12), $\mathbf{q}(t)$ in Eq.(11) satisfies Eq.(2).

Here, the relation between constraint force \mathbf{f}_n and friction force \mathbf{f}_t is shown in the following equation with coefficients of sliding friction.

$$\begin{aligned} \mathbf{f}_t &= \mathbf{K} \mathbf{f}_n, \quad \mathbf{K} = \text{diag}[K_1, K_2, \dots, K_p] \quad (13) \\ 0 &< K_i < 1, \quad (i = 1, 2, \dots, p) \end{aligned}$$

Therefore, Eq.(11) translate into the following equation.

$$\begin{aligned} &M(\mathbf{q})\ddot{\mathbf{q}} + \mathbf{h}(\mathbf{q}, \dot{\mathbf{q}}) + \mathbf{g}(\mathbf{q}) + D\dot{\mathbf{q}} \\ &= \boldsymbol{\tau} + (\mathbf{J}_c^T - \mathbf{J}_t^T \mathbf{K}) \mathbf{f}_n \end{aligned} \quad (14)$$

2.2 Derivation of reaction force with elbow-bracing

In this section, we introduce the method of deriving constraint force \mathbf{f}_n . First, eliminating $\ddot{\mathbf{q}}$ from Eqs.(11), (12), and defining $(\partial C / \partial \mathbf{q}^T) M^{-1} (\partial C / \partial \mathbf{q}^T)^T$ as M_c , we can get the following equation.

$$\begin{aligned} M_c \mathbf{f}_n &= \left\| \frac{\partial C}{\partial \mathbf{r}^T} \right\| \left(\frac{\partial C}{\partial \mathbf{q}^T} \right) M^{-1} (\mathbf{J}_t^T \mathbf{K} \mathbf{f}_n + D\dot{\mathbf{q}} + \mathbf{h} \\ &+ \mathbf{g} - \boldsymbol{\tau}) - \left\| \frac{\partial C}{\partial \mathbf{r}^T} \right\| \dot{\mathbf{q}}^T \left[\frac{\partial}{\partial \mathbf{q}} \left(\frac{\partial C}{\partial \mathbf{q}^T} \right) \right] \dot{\mathbf{q}} \end{aligned} \quad (15)$$

Moreover, by using following definitions,

$$\mathbf{B} = \left\| \frac{\partial C}{\partial \mathbf{r}^T} \right\| \left(\frac{\partial C}{\partial \mathbf{q}^T} \right) M^{-1}, \quad (16)$$

$$\mathbf{a} = \mathbf{B} \{ D\dot{\mathbf{q}} + \mathbf{h} + \mathbf{g} \} - \left\| \frac{\partial C}{\partial \mathbf{r}^T} \right\| \dot{\mathbf{q}}^T \left[\frac{\partial}{\partial \mathbf{q}} \left(\frac{\partial C}{\partial \mathbf{q}^T} \right) \right] \dot{\mathbf{q}}, \quad (17)$$

Eq.(15) can be into,

$$M_c \mathbf{f}_n = \mathbf{B} \mathbf{J}_t^T \mathbf{K} \mathbf{f}_n - \mathbf{B} \boldsymbol{\tau} + \mathbf{a}. \quad (18)$$

Moreover, we define the following matrix \mathbf{A} included in Eq.(18).

$$\mathbf{A} = M_c - \mathbf{B} \mathbf{J}_t^T \mathbf{K} \quad (19)$$

By inputting Eq.(19) to Eq.(18), we can get Eq.(1). The relation between constraint force \mathbf{f}_n and input torque $\boldsymbol{\tau}$ is expressed as algebraic equation. Because \mathbf{f}_n is p dimensions vector and $\boldsymbol{\tau}$ is n dimension vector, $\boldsymbol{\tau}$ that achieves \mathbf{f}_n has constraint redundancy.

2.3 Simultaneous equation of robot and motor

A current of motor is expressed as a vector \mathbf{I} . We put in a dynamics of motor to Eq.(14) and get the following equation.

$$\begin{aligned} &(M(\mathbf{q}) + \mathbf{J}_m)\ddot{\mathbf{q}} + \mathbf{h}(\mathbf{q}, \dot{\mathbf{q}}) + \mathbf{g}(\mathbf{q}) + (D + D_m)\dot{\mathbf{q}} \\ &= \mathbf{K}_m \mathbf{I} + (\mathbf{J}_c^T - \mathbf{J}_t^T \mathbf{K}) \mathbf{f}_n \end{aligned} \quad (20)$$

Here, \mathbf{J}_m is a diagonal matrix of inertia moment of motor's rotor, D_m is a coefficient matrix of viscosity resistance, \mathbf{K}_m is a torque constant matrix of motor. As the relation between Eq.(2) and Eq.(11), $\ddot{\mathbf{q}}$ that satisfy Eq.(12) and $\ddot{\mathbf{q}}$ in Eq.(20)

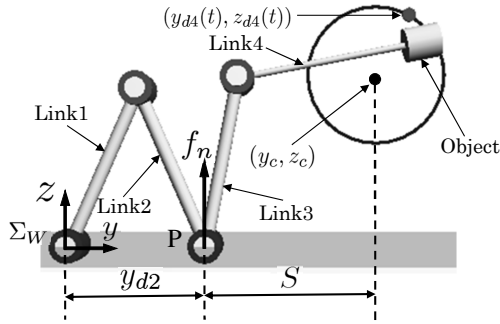


Fig. 2. Simulation model

are same value, $q(t)$ in Eq.(20) satisfy Eq.(2). Moreover, the relation between applied voltage and current of motor like

$$L \frac{dI}{dt} = v - RI - K_m \dot{q}. \quad (21)$$

Eq.(21) is combined with Eqs.(12), (20). So, equation of motion of n links manipulator that is subject to constraint at p points including the dynamics of motor is expressed as

$$\begin{bmatrix} M + J_m & -(J_c^T - J_t^T K) & 0 \\ \frac{\partial C}{\partial q^T} & 0 & 0 \\ 0 & 0 & L \end{bmatrix} \begin{bmatrix} \ddot{q} \\ f_n \\ dI/dt \end{bmatrix} = \begin{bmatrix} K_m i - h - g - (D + D_m) \dot{q} \\ -\dot{q}^T \left[\frac{\partial}{\partial q} \left(\frac{\partial C}{\partial q^T} \right) \right] \dot{q} \\ v - RI - K_m \dot{q} \end{bmatrix}. \quad (22)$$

3 POSITION/FORCE CONTROL WITH CONSTRAINT REDUNDANCY

When the dynamics of motor is not considered, from Eq.(1), the solution τ that achieve desired constraint force f_{nd} is expressed as

$$\tau = B^+(a - Af_{nd}) + (I - B^+B)l. \quad (23)$$

But, B^+ is pseudo inverse matrix. $\text{rank}(I - B^+B)$ equal $n - p$. Because $I - B^+B$ is non-dimensional matrix, l has dimensions of torque. We consider l new input, and l can be used to track target trajectory of hand r_d and control bracing position through null-space $I - B^+B$ of B . By the quality of pseudo inverse matrix, adding any value to l has no effect on achieving f_{nd} . So, we can decouple the task of tracking trajectory from the task of achieving f_{nd} .

Here, a method of determination of l is shown. In the simulation of this report, we use one degree of freedom to force control of elbow, one degree of freedom to position control of elbow and two degrees of freedom to position control of hand and control 4 links manipulator with four degrees of

freedom.

$$l = \tilde{j}_{2y}^T [K_{p2y}(y_{d2} - y_2) + K_{d2y}(\dot{y}_{d2} - \dot{y}_2)] + J_4^T [K_{p4}(r_{d4} - r_4) + K_{d4}(\dot{r}_{d4} - \dot{r}_4)] \quad (24)$$

Here, \tilde{j}_{2y}^T is first column of column vectors that compose \tilde{J}_2^T that is defined in Eq.(4). And K_{p2y} and K_{d2y} are control gains of position and velocity in y axis direction of 2nd link that is shown in Fig.2, J_4 is Jacobian matrix of 4th link and K_{p4} and K_{d4} are control gain matrices of position and velocity of 4th link.

Eq.(23) can be shown in the case that robots are driven by DD motor, but input of usual motor is voltage input. In this report, the following equation is used instead of a controller of Eq.(23).

$$v = K_v [B^+(a - Af_{nd}) + (I - B^+B)l] \quad (25)$$

4 SIMULATION OF TRACKING HAND TRAJECTORY

In this chapter, we report the simulation of 4 links manipulator. a model that is used in this simulations is shown in Fig. 2. Link's weight is $m_i = 1.0$ [kg], link's length is $l_i = 0.5$ [m], viscous friction coefficient of joint is $D_i = 2.9$ [N · m · s/rad], torque constant is $K_i = 0.2$ [N · m/A], resistance is $R_i = 0.6$ [Ω], inductance is $L_i = 0.1$ [H], inertia moment of motor is $I_{mi} = 1.64 \times 10^{-4}$ [kg · m²], reduction ratio is $k_i = 3.0$ and viscous friction coefficient of reducer is $d_{mi} = 0.1$ [N · m · s/rad] ($i = 1, 2, 3, 4$).

Hand target trajectory is shown as the following equations.

$$y_d(t) = 0.2 \cos \frac{2\pi}{10} t + y_c \quad (26)$$

$$z_d(t) = 0.2 \sin \frac{2\pi}{10} t + z_c \quad (27)$$

4.1 Effectiveness of bracing elbow

In this section, we show effectiveness of bracing elbow. Energy consumption and accuracy of hand control are used as evaluation index. And derivation method of energy consumption is shown as follows. Energy consumption of i -th link of manipulator is represented as the following equations during $0 \sim T$ [s].

$$E_i(T) = \int_0^T v_i(t) I_i(t) dt \quad (28)$$

$$E_{sum}(T) = \sum_{i=1}^4 E_i(T) \quad (29)$$

Here, we assume the second joint as elbow, and we ran two simulations. The contents are that a elbow of manipulator is subject to constraint and is not subject to constraint. Center coordinate of target trajectory in Fig.2 is

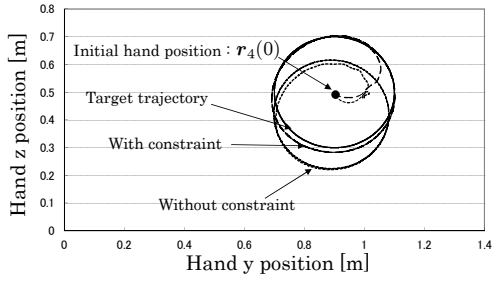


Fig. 3. Position time profile of hand

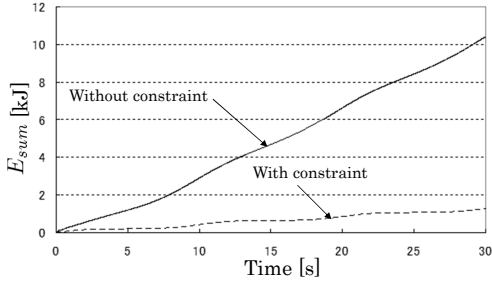


Fig. 4. Comparison of energy consumption defined by Eq.(29)

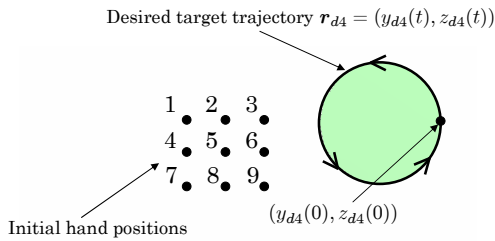


Fig. 5. Initial hand positions

$(y_c, z_c) = (0.9, 0.5)[m]$, initial hand position is $(0.9, 0.5)$ and initial bracing position is $(0.4, 0)$. Graphs of hand trajectory and energy consumption from $t = 0[s]$ to $t = 30[s]$ in the case that the elbow is subject to constraint and is not subject to constraint are shown as Figs.3, 4. From Fig.3, the accuracy of elbow is better by bracing elbow. And Fig.4, energy consumption reduced by 1/10. So, the motion of bracing elbow is effective.

4.2 Attribution of tracking hand trajectory and initial value dependence

A Target trajectory of hand and the initial positions are shown in Fig.5. We prepared nine positions as initial hand position. Because we consider that total weight of links is 4[kg], we set $f_{n2d} = 30$ for a desired value of constraint force. y_{2d} in Eq.(24) is 0.4[m] and gains are $K_{p4} = \text{diag}[300, 300]$, $K_{d4} = \text{diag}[100, 100]$, $K_{p2y} = 150$, [N/m] and $K_{d2y} = 75$, [Ns/m]. Initial elbow bracing

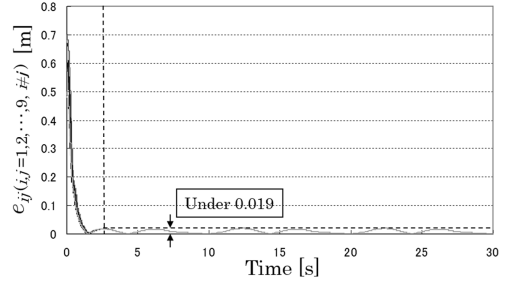


Fig. 6. Error of the hand

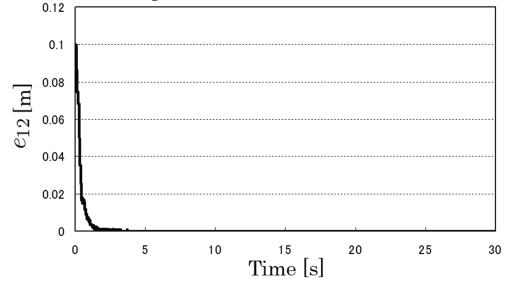


Fig. 7. Error profile between the trajectory started from initial point1 in Fig.5 and the trajectory started from point2

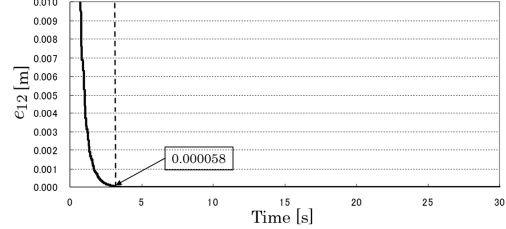


Fig. 8. Expanded error profile in Fig.7

position is $(0.4, 0.0)$ in all cases.

Here, Errors e between a target trajectory and hand trajectories are defined as the following equation.

$$e(t) = \sqrt{(y_{d4} - y_4)^2 + (z_{d4} - z_4)^2} \quad (30)$$

Errors between hand trajectories started from i and j in initial positions 1 ~ 9 are defined as the following equation.

$$e_{ij}(t) = \sqrt{(y_{4i} - y_{4j})^2 + (z_{4i} - z_{4j})^2} \quad (i, j = 1, 2, \dots, 9, i \neq j) \quad (31)$$

But, i and j are 1 ~ 9 in Fig.5.

In Fig.6, the errors between hand trajectories started from i and j in initial positions 1 ~ 9 are much the same and less than 0.019[m] after 3[s]. Next, the error $e_{12}(t)$ of trajectory started from 1 and 2 is shown in Fig.7, and an extended figure of Fig.7 is shown in Fig.8. The error is less than 5.8×10^{-5} after 3[s]. Cases of other errors of trajectories are same, so we calculated that there is no effect for the difference of initial values after 3[s].

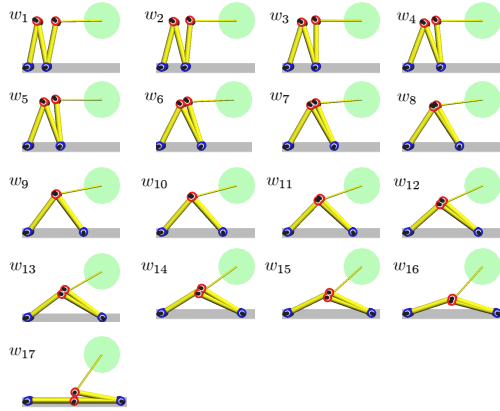


Fig. 9. Desired elbow-bracing position in simulation: $w_1 : y_{d2} = y_2(0) = 0.20$, $w_2 : y_{d2} = y_2(0) = 0.25$
 $w_3 : y_{d2} = y_2(0) = 0.30$, $w_4 : y_{d2} = y_2(0) = 0.35$
 $w_5 : y_{d2} = y_6(0) = 0.40$, $w_6 : y_{d2} = y_2(0) = 0.45$
 $w_7 : y_{d2} = y_9(0) = 0.50$, $w_8 : y_{d2} = y_2(0) = 0.55$
 $w_9 : y_{d2} = y_2(0) = 0.60$, $w_{10} : y_{d2} = y_2(0) = 0.65$
 $w_{11} : y_{d2} = y_2(0) = 0.70$, $w_{12} : y_{d2} = y_2(0) = 0.75$
 $w_{13} : y_{d2} = y_2(0) = 0.80$, $w_{14} : y_{d2} = y_2(0) = 0.85$
 $w_{15} : y_{d2} = y_2(0) = 0.90$, $w_{16} : y_{d2} = y_2(0) = 0.95$
 $w_{17} : y_{d2} = y_2(0) = 1.00$, where y_{d2} is given by Eq.(24)

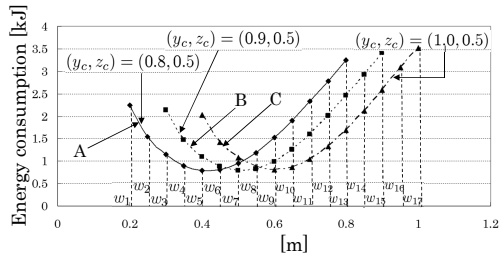


Fig. 10. Evaluation of energy consumption($M=0.0$)

4.3 Optimization of elbow bracing position

In this section, optimization of elbow bracing position is shown. From previous simulation, because we calculated that there is no effect for the difference of initial values after 3[s], elbow bracing position is optimized by energy consumption $E_{sum}^*(T)$ after $t = 3$ [s].

$$E_i^*(T) = \int_3^T v_i(t) I_i(t) dt \quad (32)$$

$$E_{sum}^*(T) = \sum_{i=1}^4 E_i^*(T) \quad (33)$$

Weight of hand's load is changed as $0.0, 0.2, \dots, 1.2$ [kg]. Central coordinates of target trajectory are defined as $(y_c, z_c) = (0.8, 0.5), (0.9, 0.5), (1.0, 0.5)$, and the three cases are shown as A, B and C. Target bracing position y_{d2} and initial bracing position $y_2(0)$ are shown from w_1 to w_{17}

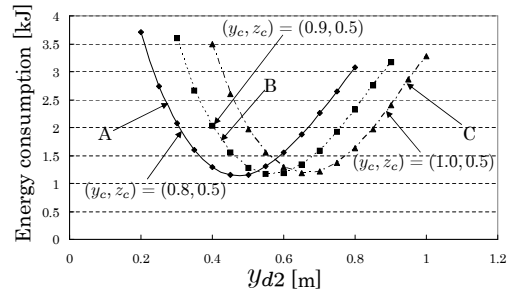


Fig. 11. Evaluation of energy consumption($M=0.2$)

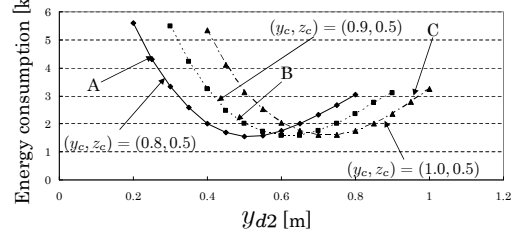


Fig. 12. Evaluation of energy consumption($M=0.4$)

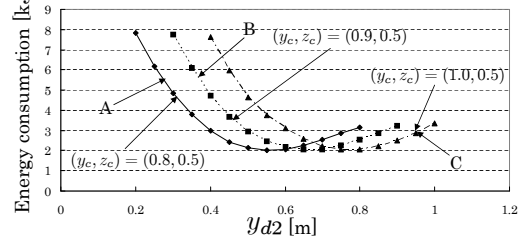


Fig. 13. Evaluation of energy consumption($M=0.6$)

in Fig.9. Because initial hand position is central coordinates of target trajectory, we set initial hand position as A(0.8,0.5), B(0.9,0.5) and C(1.0,0.5) for each trajectories.

Fig.10 is a case that hand's load is zero, and a vertical axis shows energy consumption that is given as Eq.(33). Bracing position of a abscissa axis in Fig.10 is a distance from a origin point of task coordinate system Σ_W to bracing position in Fig.2. From Fig.10, In the case of $M = 0$, the center coordinates of target trajectory move to A : (0.8, 0.5), B : (0.9, 0.5) and C : (1.0, 0.5), optimal bracing positions are 0.4, 0.5 and 0.6[m] in each cases. A, B and C in Fig.10 correspond to A, B and C that show the above positions of target trajectory. From Fig.10, as the center coordinates of target trajectory move to positive direction of y axis like A, B and C, optimal bracing position also move to positive direction of y axis.

Next, we change the weight M of object that is attached on the hand from 0.2[kg] to 1.2[kg] in steps of 0.2[kg], and we run simulations by changing bracing position like Fig.9 for each cases. Graphs of energy consumption for the change of bracing position and the center coordinate are shown in

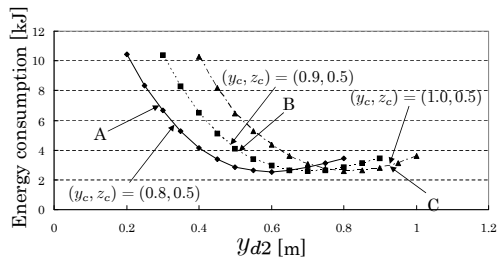


Fig. 14. Evaluation of energy consumption($M=0.8$)

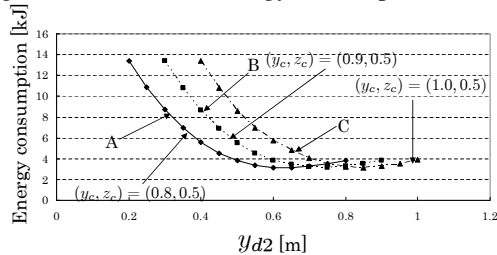


Fig. 15. Evaluation of energy consumption($M=1.0$)

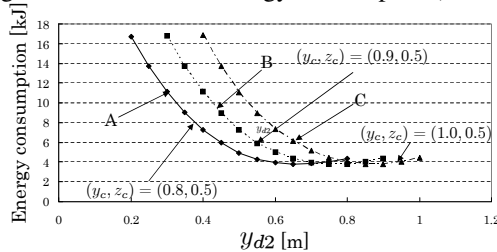


Fig. 16. Evaluation of energy consumption($M=1.2$)

Figs.11-16.

Here, the distance between the center coordinates and the bracing position in Fig.2 is defined as S , and S equals $y_c - y_{d2}$. Optimal bracing position S in the case that the center coordinate is A is $S = 0.8 - 0.4 = 0.4$ [m] in Fig.10. In Fig.11, because energy consumption is lowest in $y_{d2} = 0.45$, $S = 0.8 - 0.45 = 0.35$. From Figs.10-16, S are 0.40 [m] ($M = 0.0$) [kg], 0.35 ($M = 0.2$), 0.30 ($M = 0.4$), 0.25 ($M = 0.6$), 0.20 ($M = 0.8$), 0.15 ($M = 1.0$) and 0.15 ($M = 1.2$).

From the above, as hand's load increase, energy consumption in the case of bracing elbow near the target trajectory is lower than others.

Forms of graphs of each energy consumptions in Figs.10-16 are horseshoe shape, and in the case that bracing position is too near to target trajectory, energy consumption increase. From Figs.10-16, as hand's load increase, it is difficult to discriminate optimal bracing position. Moreover, from Fig.10, minimum energy consumption in the case of $M = 0$ is 0.8 [kJ] regardless of A, B and C. From Fig.11, minimum energy consumption is 1.1 kJ ($M=0.2$), and from Fig.12, minimum energy consumption is 1.6 ($M=0.4$). Similarly, min-

imum energy consumptions are 2.0 ($M=0.6$), 2.5 ($M=0.8$), 3.1 ($M=1.0$) and 3.8 ($M=1.2$). From the above, as hand's load increase, minimum energy consumption increase.

From Figs.10-16, when bracing position y_{d2} move from $w_1 : 0.2$ to $w_{17} : 1.0$, the difference between maximum and minimum energy consumption increase as increasing hand's load. The difference of energy consumption depended on bracing position is so noticeable as to increase hand's load, and the effect of optimizing bracing position is so great as to grasp heavy load.

5 CONCLUSION

In this paper, advantages of constrain motion regarding accuracy of tracking hand trajectory was considered by comparing motion of bracing elbow to motion of no bracing elbow. Then, we showed that accuracy of tracking trajectory improved and energy consumption decrease by bracing elbow. Moreover, we showed that bracing position that minimize energy consumption changed depended on position of target trajectory and weight of hand's load. In the future, we will perform optimizing control of bracing position in real time from the results of this simulations.

REFERENCES

- [1] G. S. Chirikjian, J. W. Burdick(1994), A Hyper-Redundant Manipulator, IEEE Robotics and Automation Magazine, 1994, pp.22-29
- [2] K. Glass, R. Colbaugh, D. Lim, H. Seraji(1995), Real-time collision avoidance for redundant manipulators, IEEE Trans. on Robotics and Automation, Vol.11,1995, pp.448-457
- [3] H. Seraji, B. Bon(1999), Real-Time Collision Avoidance for Position-Controlled Manipulators, IEEE Trans. on Robotics and Automation, Vol.15, No.4, 1999, pp.670-677
- [4] S. Hirose, R. Chu(1999), Development of a light weight torque limiting M-Drive actuator for hyper-redundant manipulator Float Arm, Robotics and Automation, 1999. Proc. of IEEE International Conference, Vol.4, pp.2831-2836
- [5] H. West, H. Asada(1985), A Method for the Design of Hybrid Position/Force Controllers for Manipulators Constrained by Contact with the Environment, Proc. of IEEE Int. Conf. on Robotics and Automation, 1985, pp.251-260
- [6] H. Hemami, B. F. Wyman(1979), Modeling and Control of Constrained Dynamic Systems with Application to Biped Locomotion in the Frontal Plane, IEEE Trans. on Automatic Control, Vol.AC-24, No.4, 1979, pp.526-535
- [7] Z. X. Peng, N. Adachi(1991), Position and Force Control of Manipulators without Using Force Sensors (in Japanese), Trans. of the Japan Society of Mechanical Engineers(C), Vol.57, 1991, pp.1625-1630